JJEES

JJEES (2019) 10 (1): 35-45
ISSN 1995-6681

Jordan Journal of Earth and Environmental Sciences

Adsorption Modeling of Cr^{+3} on Volcanic Tuff-Based Geopolymer

Kamel Al-Zboon[1], Bashar Al-Smadi[2],
Mohammad Al-Harahsheh[3], Sajedh Al-Khawaldh[2]

[1]Al-Balqa Applied University, Al-Huson University College,Department of Environmental Engineering, Irbid, Jordan
[2]University of Jordan, Department of Civil Engineering, Faculty of Engineering and Technology, Amman, Jordan
[3]Jordan University of Science and Technology, Faculty of Engineering, Department of Chemical Engineering, Irbid, Jordan

Received 30 June, 2018; Accepted 3 February, 2019

Abstract

In the current work, geopolymer was synthesized from volcanic tuff and was then used as a sorbent for Cr^{+3} from aqueous solutions. An adsorption batch experiment was conducted to study the factors affecting the adsorption process. The obtained results showed a high removal efficiency of geopolymer (96 %) against 70 % for the volcanic tuff with an uptake capacity of 21.24 and 14.76 mg/g for both materials, respectively. The removal efficiency increased with increasing the pH up to 5, geopolymer dosage, contact time up to thirty minutes, temperature, and the decrease of Cr^{+3} initial concentration in the studied ranges. The validity of the isotherm models to the experimental data can be ranked in the order of Langmuir > Temkin > Frundilch > Dubinin–Radushkevich. The kinetic study showed that the second order model provided the best fit with R^2 of 0.97 against 0.44 and 0.62 for the first order and the intra-particle model. The sorption process can be described as endothermic, monolayer, physical, and of a high ion affinity to the surface of the geopolymer. The results obtained buttressed the applicability of using a volcanic tuff-based geopolymer for the Cr^{+3} removal as a low-cost natural material at low concentrations.

Keywords: Geopolymer, Volcanic tuff, Adsorption, Chromium, isotherm, kinetic modeling.

1. Introduction

Chromium is generated as waste stream from numerous industries including textile, leather, pigments and paints, metal finishing, chromium alloy, the ceramic and glass industry, production of catalysts, photography, fungicides, refractories, drilling mud, and corrosion control (Krishna and Sree, 2013; Jacobs and Testa, 2004). Poor housekeeping of Cr^{+3} waste leads to the spill and leakage into the environment which causes serious contamination to the soil and groundwater (Jacobs and Testa, 2004). The ingestion of 1–5 g of chromate results in severe effects including gastrointestinal disorders, haemorrhagic diathesis, and convulsions (WHO, 2003). Mutagenicity effects include increase in incidences of genotoxic effects such as sister chromatid exchanges and chromosomal aberrations (Janus and Krajnc, 1990; WHO, 2003). Due to its impact on human health, the California Office of Environmental Health Hazard Assessment (OEHHA) recommended a public health goal (PHG) of 2.5 mg/l for total chromium and 0.02 mg/l for Cr(VI) (Jacobs and Testa, 2004). Stricter standards were set by EPA with a drinking water level of 0.10 mg/l for total chromium (EPA, 2010).

Traditional removal methods of chromium include, but are not limited to: ion exchange, revers osmoses, adsorption, membrane filtration, soil flushing, and electrokinetics (Hawley et al., 2004). Chromium transformation options include: chemical (oxidation-reduction, sorption, and precipitation), biological and physical transformation. Although precipitation is the most commonly used method, the main drawback of this method is the formation of high quantity of sludge (Pansini et al., 1991). Recent researches focus on the use of low cost treatment as an attractive option for Cr removal such as coconut fibers waste (Mohan et al., 2006), powdered marble waste (Ghazy et al., 2010), waste newspaper (Dehghani et al., 2015), eggshell (Ghazy et al., 2008), rice husk (Bansal et al., 2008), fruit skins (Rane et al., 2008), saw dust (Bansal et al., 2008), activated neem leaves, activated tamarind seeds, activated fly ash, sawdust, (Gupta and Babu, 2008) and geopolymers (Chen et al., 2016).

Geopolymer showed superior physical, chemical, and mechanical properties such as compressive strength, thermal insulation, low permeability, acid and fire resistance, quick setting, freeze-thaw cycle resistance, and low heavy metal mobility contained within the geopolymeric structure (Al-Zboon et al., 2011). Such properties nominated it successfully to be used for many engineering applications including: cements and high tensile and compression strength concrete, heat resistance concretes, resin, paint, binder, grout, and in ceramic industries. In the environmental field, geopolymer was used for the removal of Cu (Al-Harahsheh et al., 2015; Cheng et al., 2012), Pb (López et al., 2014; Al-Zboon et al., 2011), Zn (Al-Zboon et al., 2016), Cs^+ (López et al., 2014), Cd (Cheng et al., 2012), cobalt (Mužeka et al., 2016), ammonium (Luukkonen et al., 2016), dyes (Li et al., 2006), and for the stabilization of radioactive materials (Hanzlicek et al., 2006).

Several researchers have investigated the possibility of producing geopolymer from different materials such as metakaoline (López et al., 2014; Hamaideh et al., 2014), fly ash (Mužeka et al., 2016, Al-Zboon et al., 2011), volcanic tuff (Al-Zboon et al., 2016), Aluminium hydroxide waste

* Corresponding author e-mail: kazboon@yahoo.com

(Onutai et al., 2015), waste glass (Christiansen, 2013), rice husk (He et al., 2013), waste foundry sand (Devi and Kumar, 2015), waste serpentine cutting (Cheng, 2003), fly ash from the incinerators of municipal solid waste (Lancellotti et al., 2011), slag (Astutiningsih and Liu, 2005) and red mud (He et al., 2013).

The heavy metal removal efficiency of geopolymer is influenced by many parameters including: pH, geopolymer dosage, contact time, contaminant initial concentration, temperature and the composition of geopolymer.

Since its discovery in Jordan in 1968, volcanic tuff opened the door for research depending on its inventive characteristics. Because of the availability, good porosity, low cost, volcanic tuff is used in numerous engineering applications such as in light-weight concrete production (Al-Zboon and Al-Zou'by, 2016), water and wastewater treatment (El-Eswed et al., 2012; Al-Zou'by et al., 2013; Ibrahim, 2001), air-pollution control (Al-Harahsheh et al., 2014), soil improvement (Al-Tabbal et al., 2016), cooling and heating systems (Sqoor et al., 2015) and heavy metal removal (Ibrahim et al., 2016).

For this study, volcanic tuff samples were collected from Jabal Aritien site located north east of Jordan. The collected samples were used for the production of geopolymer and for Cr^{+3} removal. To the authors' best knowledge, this is the first time volcanic tuff- based geopolymer is used for Cr removal. The results of this study may open the door for future researches regarding the production of geopolymer from natural materials to be used for many environmental applications such as gases and heavy metal removal. The possible parameters affecting the adsorption process were considered. Adsorption isotherm, kinetic, and the thermodynamic behavior of the adsorbate were also investigated.

2. Materials and Methodology

2.1. Materials

A volcanic tuff sample of two cubic meter volume was obtained from Jabal Aritin (30 km east of Al Mafraq city), one of the identified volcanic tuff sites in Jordan. The collected sample was reduced to the required volume by cone and quartering dividing method. The obtained sample was sieved, and the sieve fraction of <45 µm was used for geopolymer production (Al-Zboon et al., 2011). Reagent grade chemicals (Nitric acid and sodium hydroxide) and chromium nitrate stock solution with a concentration of 1000 ppm was obtained from Merck- Germany.

2.2. Instrumentation

X-ray diffraction (XRD) analysis for feed material (tuff) and the product (geopolymer) samples were performed using (SHIMADZU-XRD-6000). The chemical composition was obtained using X-ray fluorescence (XRF) spectrometer (SHIMADZU-XRF-1800). Chromium concentration in the aqueous solution was measured using Inductively Coupled Plasma Optical Emission Spectrometer (ICP-OES) (SHIMADZU-ICPS-7510). The pH measurements were performed using pH meter model inoLab® pH 7110 from WTW. A water bath shaker equipped with a digital thermostat was used to regulate the temperature to perform the sorption tests at different temperatures.

2.3. Synthesis of Geopolymer

The geopolymer samples were produced according to the procedure followed by (Al-Zboon, et al., 2011), as demonstrated in Figure 1. A certain mass of volcanic tuff with the size of <45 µm was mixed with NaOH (14 M) with the ratio of 1:1.25, where NaOH is considered the best activator (Abdul Rahim et al., 2014). The vibration process will de-foam the geopolymer matrix. To enhance the dissolution of material in the NaOH solution, ultrasonication was used (Álvarez et al., 2008).

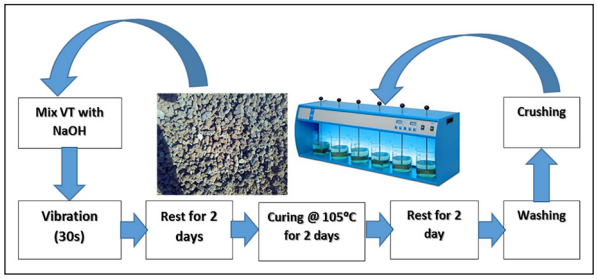

Figure 1. Procedure for the synthesis of geopolymer

High-temperature curing (105 ºC) will accelerate the formation of geopolymer and increase its strength. It was reported that the temperature range of 60-100 ºC yielded the highest strength under compression (Al Bakri et al., 2012); however, the higher temperature did not affect the compressive strength (Rangan, 2008). After geopolymerization, the geopolymer was washed with water to remove the excess of NaOH. The process of washing continued until reaching constant pH of the washing water, which was achieved after three washing times. The produced geopolymer was ground to 100 % < 200µm to be used for further adsorption, isotherm, and kinetic studies.

2.4. Adsorption Tests

A Jar test (model B-KER) with six jars made by Philipps & Bird was used to perform the adsorption tests. Specific geopolymer dosage (0.25 g) was added to the batch containing different concentrations of chromium (10-160 ppm), at different pH (1 - 6), and variable contact times (5 – 180 min). The temperature effect on adsorption behavior was studied at 25, 35, and 45 °C. After mixing; a liquid sample was separated from the solution through decantation followed by filtration.

2.5. Adsorption Performance

Three indicators were used to evaluate the performance of adsorption; these are: uptake capacity (q), efficiency (E), and Partition Coefficient (k). These indicators were calculated according to equations 1-3 below (Al-Zboon et al., 2016).

$$E = \frac{C_0 - C_e}{C_0} \times 100\% \quad \text{..... (1)}$$

$$q = \frac{(C_0 - C_e) \times V}{m} \quad \text{..... (2)}$$

$$K_d = \frac{(C_0 - C_e) \times V}{C_e \times m} \ (\text{ml/g}) \quad \text{..... (3)}$$

Where C_o is Cr^{+3} initial concentration of (ppm), C_e is the equilibrium Cr^{+3} concentration (ppm), q is Cr^{+3} uptake (mg

Cr/g of geopolymer), V is the solution volume (liters) and m is the mass of the geopolymer (dosage) (g).

2.6. Modeling of Adsorption Isotherms

Four models were tested to describe the adsorption of Cr^{+3} on the geopolymer mass. These are Langmuir's, Freundlich's, Dubinin–Radushkevich, and Temkin model. These models explained the adsorption process based on the models' assumption. Langmuir assumed a homogenous and monolayer adsorption process, whereas, Freundlich's model assumes a heterogeneous and multilayer adsorption (Foo and Hameed, 2010). Dubinin–Radushkevich's model is used to express the adsorption mechanism with a Gaussian energy distribution onto a heterogeneous surface (Dada et al., 2012). Temkin's model is based on the fact that the heat of adsorption of all molecules in the layer would decrease linearly as a function of temperature (Dada et al., 2012). The fitness of the applied models was tested by comparing the experimental data with the model predicted results.

2.7. Error Analysis

Mean Square Error (MSE) and Chi-square test (χ^2) were used as error evaluation parameters to evaluate the degree of models' fitness to the experimental data. The following equations were used for this purpose (Sampranpiboon et al., 2014):

$$MSE = \frac{1}{n}\sum(q_{exp} - q_{cal})^2 \quad \text{..... (4)}$$

$$\chi^2 = \frac{\sum(q_{exp.} - q_{cal.})^2}{q_{cal}} \quad \text{..... (5)}$$

where q_{exp} and q_{cal} are the experimental and calculated uptake capacities in mg/g.

2.8. Adsorption Kinetics

The kinetics of chromium adsorption on the synthesized geopolymer was modeled using pseudo-first-order (Equation 6) Lagergren's pseudo second order (Equation 7) and the intraparticle diffusion (Equation 8) models (Amenaghawon et al., 2013.):

$$Ln(q_e - q_t) = Lnq_e - k_1 t \quad \text{..... (6)}$$

$$\frac{t}{q_t} = \frac{1}{k_2(q_e)^2} + \frac{t}{q_e} \quad \text{..... (7)}$$

$$q_t = k_3(t)^{0.5} + I \quad \text{..... (8)}$$

where q_e and q_t stand for adsorption capacities at equilibrium and at contact time t (mg/g), k_1, K_2, K_3 are the rate constants for pseudo-first-order, Lagergren's pseudo second order and the intraparticle diffusion models , respectively (1/min) retrieved by plotting a graph of $\ln(q_e - q_t)$ versus t, t/q versus t, and q_t versus $t^{0.5}$, respectively.

2.8. Thermodynamic Calculations

To be able to calculate the thermodynamic parameters of chromium adsorption on the geopolymer, the adsorption tests were carried out at three temperatures (25, 35, and 45 ºC) and at three pH values (3, 4, and 5). The enthalpy (ΔH^o, kJ/mol), and entropy (ΔS^o, kJ/mol.K) were calculated using the following equation (Misra et al., 2003):

$$\ln K_d = (\Delta S^o/R) - (\Delta H^o/RT) \quad \text{..... (9)}$$

where T is the temperature (Kelvin), R is gas constant. A plot of ln K_d versus 1/T yields a slope of $\Delta H^o/R$ and an intercept of $\Delta S^o/R$,

The delta Gibbs free energy (ΔG^o, kJ/mol) was obtained according to Equation 10 below:

$$\Delta G^o = \Delta H^o - T\Delta S^o \quad \text{..... (10)}$$

3. Results and Discussion

3.1. Characteristics of the Natural and Synthesized Materials

The chemical and mineralogical composition of the raw volcanic tuff and the geopolymer were reported previously (Al-Zboon et al, 2016). The volcanic tuff is zeolite rich containing mainly phillipsite and chabazite minerals as main zeolite phases. These phases disappeared after geopolymerization, whereas, sodalite appeared as a new phase in the geopolymer structure. The main elements present in the volcanic tuff were Ca, Si, Mg, Al, and Fe; after geopolymerization, the sodium content increased by factor of 7 as where it incorporated in the geopolymer structure (Al-Zboon et al., 2016).

3.2. Performance of Volcanic Tuff and Geopolymer

In order to determine the benefit of using geopolymer instead of the volcanic tuff used for Cr removal, both materials were used for Cr adsorption with an initial concentration of 100 ppm, adsorbent dosage = 0.25 g, pH=5 at a temperature of 25 °C. It was found that the percentage uptake for volcanic tuff was 70.38 % against 93.65 % for geopolymer which indicated an improvement of 33 % in removal efficiency under the specified experimental conditions. Similarly, the uptake capacity increased from 14.76 to 19.3 mg Cr /g of volcanic tuff and geopolymer, respectively. Al-Zboon et al. (2016) found that the geopolymrization succeeded in producing additional pores in comparison with the raw tuff, which explains the higher adsorption capability of geopolymer. Balan et al. (2009), used Sphagnum moss peat for Cr^{+3} removal, and they obtained an uptake capacity of 18.6 mg Cr^{+3} /g of peat. Tangjuank, et al. (2009) prepared activated carbon from cashew nut shells and obtained 13.93 mg/g of Cr^{+3} uptake capacity. A lower uptake capacity was obtained by using two sources of coal (Lakhra and Thar coalfields) with the maximum Cr^{+3} uptake ranging from 2.61- 2.55 mg/g (Anwar, et al., 2009). Dam silt provided a very low adsorption capacity of 0.97 mg/g Cr^{+3} (Ouadjenia-Marouf et al., 2013). A synthesized Amberlite (IR 120 Resin) showed higher adsorption capacity toward Cr^{+3} which provided 142.86 mg Cr^{+3} /g of the resin (Meshram et al., 2012). Also, polystyrene and styrene/acrylonitrile copolymer provided a high uptake capacity up to 37.8 and 37.2 mg/g, respectively (Kanwal et al., 2012). Al Dwairi (2017) achieved a higher removal efficiency for Cr^{+6} using natural zeolitic tuff (56.3mg/g), and the smaller the particles' size, the higher the removal efficiency.

This comparison indicates that the produced geopolymer provides a high removal efficiency in comparison with a natural material which buttressed the benefit of using it for heavy metal removal.

3.3. Effect of pH:

The impact of pH on the adsorption behavior of Cr on the geopolymer was studied in the pH range of 1-7. Figure 2 below shows that the removal efficiency and the

uptake capacity increased sharply as pH increased up to 5; afterwards, it decreased slightly in the studied range. The max removal efficiency was 96 % with a max uptake of 19.2 mg/g. As pH increases, the surface of the geopolymer becomes negatively charged which enhances the positive ions of Cr to contact the geopolymer surface decreasing the repulsion forces in the system and subsequently enhancing the adsorption process (Meroufel et al., 2013). The decrease in the Cr^{+3} adsorption at the low pH can be attributed to the competition between H^+ ions and Cr^{+3} ions for the adsorption sites (Nikagolla et al., 2013).

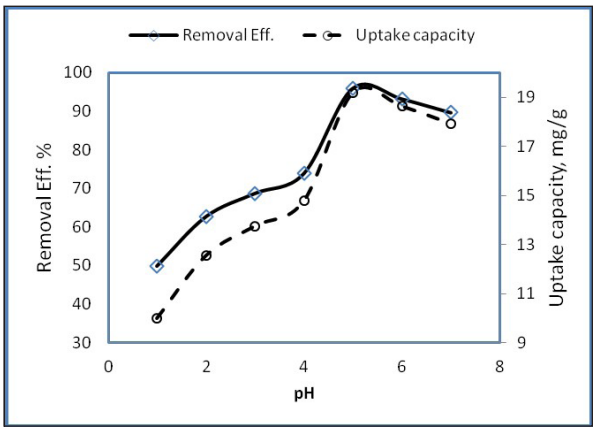

Figure 2. Impact of pH on Cr^{+3} adsorption (C_0=100 ppm, dosage=0.25g, T=25ºC, time=120 min.)

At a higher pH (>5) chromium hydroxide starts to precipitate, making true adsorption studies impossible (Kanwal et al., 2012). It was reported that the mechanism of removal appears to be ion exchange of Cr $(OH)^{2+}$ at pH≤ 6.0 and adsorption on zeolite surface of fine $Cr(OH)_3$ precipitate at pH> 6.0 (Al-Haj-Ali and Marashdeh, 2014). Bellú et al. (2008) found that the adsorption of Cr^{+3} on Grain–less Stalk of Corn increased with the increasing of pH, and there is no adsorption of Cr^{+3} at pH < 3. Balan et al. (2009) found that at a pH < 2.0, the Cr^{+3} adsorption was insignificant but increased rapidly with the increase of pH value reaching a maximum adsorption in the range of 4.0–5.5.

Tofan et al. (2015) found that the maximum removal of Cr^{+3} by alizarin pretreated hemp occurred at pH 5.8. Meshram et al. (2012) found that the extraction of Cr^{+3} from Amberlite Resin was found to be invariant in the pH range from 1.0 to 4.5; however, it decreases with a further increase in pH. Kanwal et al. (2012) reported that pH substantially affects the adsorption of Cr^{+3} on Synthetic Polymers, Copolymers and the maximum adsorption takes place at pH = 7. Tangjuank et al. (2009) used a lower pH (3.5) as the optimum for Cr^{+3} uptake on activated carbon prepared from cashew nut shells.

The best pH for the adsorption process depends on many interactive parameters such as the type, physiochemical properties, structure, and the mineral compositions of the adsorbent.

3.4. Effect of Geopolymer Dosage:

The effect of geopolymer dosage on the removal efficiency was investigated in the range of 0.03 – 1.00 g, at pH (5), temperature (25 °C), Cr concentration (100 ppm) and contact time (120 min.). Figure 3 shows that the removal efficiency increased from 67.33 to 98.93 % when the geopolymer dosage increased from 0.03 to 1.00 g. As the geopolymer dosage increased, the available pores and surface area for bending increased which also increased the opportunity for Cr ions to connect with the geopolymer surface. Many researchers reported that the removal efficiency increased with the increase of geopolymer dosage (Tangjuank et al., 2009; Balan et al., 2009; Al-Zboon et al., 2011; Al-Harahsheh et al., 2015; Odeh et al., 2015; Al-Zboon et al., 2016,).

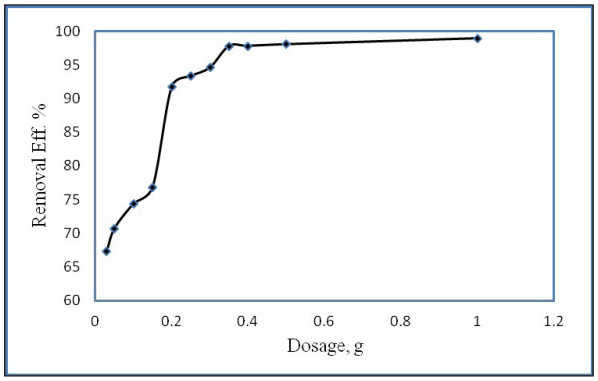

Figure 3. Impact of geopolymer dosage on Cr^{+3} adsorption (C_0= 100 ppm, pH=5, T=25 ºC, time =120 min.)

Krishna and Sree (2013) reported that the removal percentage of chromium increased from 58.25 % to 90.07 % with the increase of the adsorbent dosage (Custard Apple Peel Powder) from 0.10 to 0.60 g.

3.5. Effect of Initial Concentration

The effect of Cr^{+3} initial concentration on its removal efficiency was studied with the initial concentration ranging between 10- 160 ppm, pH=5, dosage of 0.25 g and a temperature of 25 °C. It was found that the removal efficiency decreased from 99.2 % at C_o of 10 ppm to 67.4 % at C_o of 160 ppm, while the uptake capacity increased from 1.98 to 21.58 mg/g for the same concentrations respectively as shown in Figure 4.

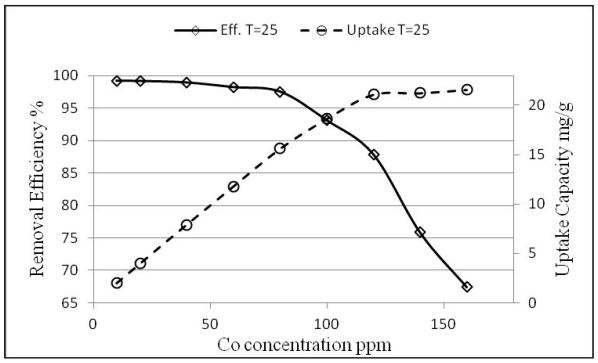

Figure 4. Effect of Cr^{+3} initial concentration on the removal efficiency (uptake capacity) by the geopolymer (pH = 5, dosage = 0.25g, T= 25 °C, time = 120 min.).

At a low concentration of Cr^{+3}, the available pores are enough to host most of the ions, whereas, at a higher concentration, some of the metal ions will not find the required pores due to the high competition on the available bending sites.

Similar results were obtained by Kanwal et al. (2012), who found that all the tested adsorbents (polystyrene, polyacrylonitrile, polymmethylmethacrylate, and

polyacrylicacid) showed a reduction in chromium removal in the concentration range of 200 - 400 ppm due to the fact that the active sites are limited and occupied with Cr^{+3} as the concentration of Cr^{+3} is increased. Yousef et al. (2015) also reported that with the gradual increase of Cr^{+3} concentration, there is a decrease in its removal by cation-exchange resin.

The increase of the Cr^{+3} concentration from 10 mg/l to 104 mg/l at pH 4 decreased the removal percentage of Cr^{+3} by Sphagnum moss peat from about 86.5 to 28.5 % (Balan, et al., 2009). Tofan et al. (2015) found that the increase in the Cr^{+3} concentration from 13 to 26 mg/l increased the breakthrough adsorption capacity of Hemp fibers from 4.2 to 6.2 mg/g and decreased the percentage of removal from 73.6 to 62.6 %. Different results were found by Tangjuank et al. (2009) who mentioned that increasing the initial Cr^{+3} concentration caused an increase in Cr^{+3} adsorbed on activated carbons due to the sufficiency of pores.

3.6. Effect of Contact Time

Figure 5 shows the removal efficiency and uptake capacity with time. It was observed that about 96 % of Cr^{+3} was adsorbed within thirty minutes, whereas, a slight improvement (0.4 %) was noticed until 180 minutes. Similarly, the uptake capacity increased with the increase of time and reached 19.18 mg/g after thirty minutes and 19.2 mg/g after 180 minutes. A longer contact time will enhance the opportunity of metal ions to bind with the adsorbent which increases the removal efficiency; whereas, when most of the metal ions bind to the geopolymer surface, any additional contact time becomes not useful. Based on this result, it can be concluded that a time of thirty minutes is feasible for the Cr^{+3} removal on geopolymer-based volcanic tuff.

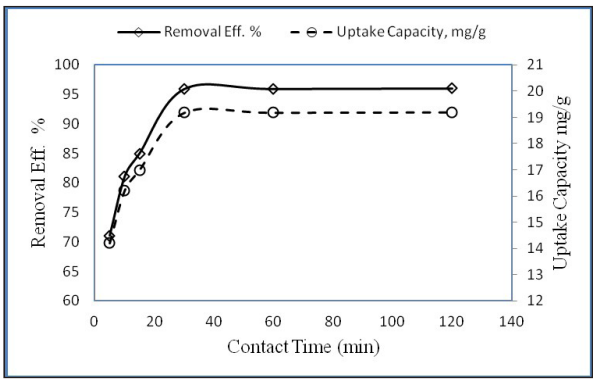

Figure 5. Impact of contact time on Cr^{+3} adsorption (pH = 5, dosage = 0.25g, T = 25 °C, C_0= 100 ppm)

Meshram et al. (2012) found that the major amount of Cr^{+3} was removed after five minutes and 99 % Cr^{+3} was removed in fifteen minutes from a 500 ppm Cr^{+3} solution. Nikagolla et al. (2013) observed that the adsorption increased rapidly and 95 % of Cr^{+3} was absorbed on natural red earth within the first ten minutes, and reached 95 % after ninety minutes.

Danielsson and Söderberg (2013) reported that the time for optimal chromium adsorption with Bauxite was determined to be forty minutes. The equilibrium contact time of sixty minutes for the adsorption of Cr^{+3} on activated carbon prepared from cashew nut shells was determined by Tangjuank et al. (2009). However, Bellú et al. (2008) found that the removal of chromium on Grain–less Stalk of Corn increased with time up to 120 minutes. and thereafter became almost constant.

3.7. Effect of Temperature

The removal efficiency increased from 89.3 to 98.6 % when the temperature increased from 25 to 45 °C at constant pH=5, dosage =0.20 g, C_0=100 ppm (Figure 6). The uptake capacity also increased from 21.24 to 24.53 mg/g for the same temperature range. The higher removal efficiency at higher temperatures is attributed to the improved diffusion through the pores of adsorbate which is known to be temperature-dependent. No significant impact of temperature on the removal efficiency at a lower concentration (<100 ppm) was observed; however, the impact of temperature was more significant at a higher concentration (Figure 7). Al-Zboon et al. (2016) found the same result confirming that at high temperature a better removal efficiency of Zn was obtained using a volcanic tuff-based Geopolymer.

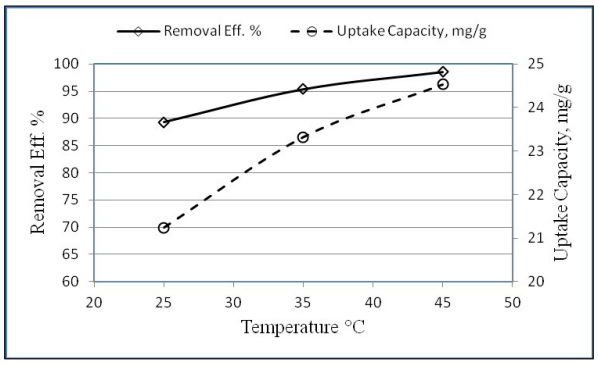

Figure 6. Impact of temperature on Cr^{+3} adsorption (pH=5, dosage = 0.25g, C_0 = 100 ppm, time = 120 min.)

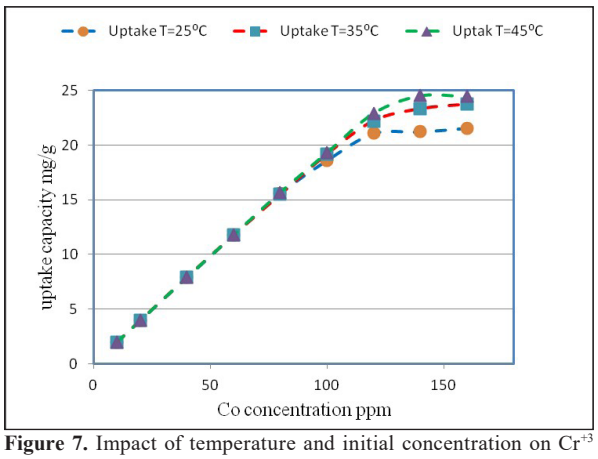

Figure 7. Impact of temperature and initial concentration on Cr^{+3} adsorption (pH=5, dosage=0.25g, T= (25, 35 and 45 °C) t= 120 min).

3.8. Adsorption Isotherm

3.8.1. Langmuir Model

The most common form of Langmuir model is given by the following linearized form (Al-Harahsheh et al., 2015):

$$\frac{1}{q_e} = \frac{1}{q_m K_L}\frac{1}{C_e} + \frac{1}{q_m} \quad \text{..... (11)}$$

where K_L is the Langmuir equilibrium constant related to the heat of adsorption and q_m is the maximum monolayer adsorption capacity.

The validity of Langmuir model was determined by plotting the experimental data, C_e versus C_e/q for the three

pH values (3, 4, and 5). The equilibrium uptake capacity (q_m), the reaction rate (k_a), and the correlation coefficient (R^2) were determined from the graph (see Table 1). It was found that q_m increased as pH and temperature increased in the studied range suggesting an endothermic adsorption behavior. The experimental data at pH = 5 and different temperatures were plotted with the calculated ones, and correlation coefficients close to 1 were obtained at temperatures of 25, 35, and 45 ºC, respectively (Figure 8). The fitness of Langmuir model suggests a monolayer homogenous adsorption process (Al-Zboon et al., 2016). At 25 ºC and pH 5, the equilibrium uptake capacity calculated by Langmuir model was 21.88 mg/g. The higher K_a values (>0.68) at pH 5 indicate a high affinity of Cr^{+3} on the geopolymer surface at this pH (Sampranpiboon et al., 2014) against a lower affinity at pH 3 and 4 where low K_a values were found.

Table 1. Calculated parameters of Langmuir isotherm model at different temperatures and pH values

Model	pH=3			pH=4			pH=5		
	R^2	q_m	Ka	R^2	q_m	Ka	R^2	q_m	Ka
T= 25	0.996	10.53	0.045	0.996	16.92	0.072	0.999	21.88	1.18
T= 35	0.997	13.19	0.054	0.998	20.24	0.089	0.999	24.24	1.03
T= 45	0.997	15.84	0.072	0.998	25.12	0.095	0.999	25.06	1.30

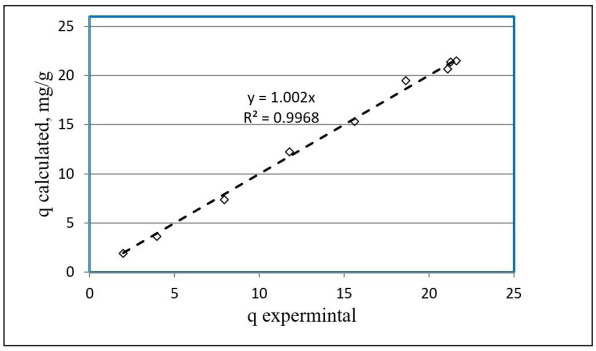

Figure 8. Correlation of calculated and experimental uptake capacity (pH=5, T=25 ºC) for Langmuir model

Balan et al. (2009) found that the isotherms data of Cr^{+3} ions adsorption on sphagnum moss peat were better described by the Langmuir model, while Meshram et al. (2012) found the adsorption of Cr^{+3} on Amberlite (IR 120 resin) following Freundlich isotherm and Langmuir models, with a maximum adsorption capacity of 142.86 mg Cr^{+3} /g resin. Nikagolla et al. (2013) reported that the experimental results of Cr^{+3} adsorption on natural red earth fit well with the Langmuir isotherm only at pH = 2, while adsorption shows a nonconformity from the Langmuir isotherm at pH >2.

The values of the dimensionless separation factor (R_L) was determined from Langmuir model at pH 5 and a temperature of 25 ºC according to the following equation (Al-Zboon et al., 2011):

$$R_L = \frac{1}{1 + K_a C_o} \quad \text{..... (12)}$$

where K_a is the Langmuir coefficient, C_o is the equilibrium concentration. The values of R_L were 0.021, 0.024, and 0.019 at temperatures of 25, 35 and 45 ºC, respectively. The values of R_L was close to zero suggesting that the adsorption is a highly advantageous and irreversible (Dada et al., 2012) and the adsorbate will not dissolve back into the solution.

3.8.2. Freundlich Model

The logarithmic form of Freundlich isotherm is expressed by the following equation (Al-Harahsheh et al., 2015):

$$\ln q_e = \ln K_F + \frac{1}{n} \ln C_e \quad \text{..... (13)}$$

where q_e is the quantity of the solute adsorbed per unit weight of adsorbent at equilibrium, C_e is the equilibrium concentration of the adsorbing compound, and K_F ($mg^{1-1/n} \cdot g^{-1} \cdot l^{1/n}$) represents the adsorption capacity when metal ion equilibrium concentration equals 1, and n represents the degree of the dependence of adsorption on equilibrium concentration

The Log q_e was plotted against Log C_e at three pH values (4, 5, 6) and temperatures (25, 35, 45 ºC) to determine the Freundlich model parameters yielding an intercept ($\log K_F$)), and a slop (1/n). The values of K_f ranged from 1.05 at pH=3 and T=25 ºC to 9.66 at pH=5 and T=45 ºC, with a significant increase as the pH and temperature increased which suggests more adsorption at higher temperatures (Donat et al., 2005). The impact of pH on K_f values was higher than the impact of temperature, where K_f values increased more than 5 times with the pH increase from 3 to 5. Its value increased only by 22-58 % as the temperature increased from 25 to 45 ºC. The n values ranged from 1.66 at pH=3 and T=35 ºC to 2.96 at pH=5 and T=25 ºC; a insignificant increasing trend with temperature. It was reported that if value 1/n <1, it indicates a normal adsorption (Dada et al., 2012). All n values >1 and <10 indicating a favorable adsorption process (Donat et al., 2005). The correlation coefficient (R^2) values ranged from 0.84 to 0.96 with a better correlation at a lower pH (Table 2). Freundlich model has less fitness with the adsorption data than the Langmuir models, which suggests that the homogenous adsorption is better at describing the process compared with heterogeneous adsorption. A higher fitness of Freundlich model at lower pH values (3, 4) may indicate that the adsorption process at this pH range has affinity to the heterogeneity and becomes homogenous at a higher pH (5). This behavior is attributed to the different adsorption sites of geopolymer with different adsorption energies at this range of pH (Nikagolla et al., 2013).

Table 2. Calculated parameters of Freundlich isotherm model at different temperatures and pH values

Temperature	pH= 3			pH =4			pH =5		
	R^2	K_f	n	R^2	K_f	n	R^2	K_f	n
25	0.96	1.05	1.99	0.96	1.85	1.99	0.84	8.13	2.966
35	0.96	1.29	1.66	0.95	2.23	1.86	0.87	8.76	1.86
45	0.95	1.66	1.94	0.95	2.61	1.7	0.86	9.66	2.61

3.8.3. Dubinin–Radushkevich Isotherm Model

The Dubinin–Radushkevich isotherm model is applied to express the adsorption process which happened onto both the homogeneous and heterogeneous surfaces (Chen, 2015). The general term of this model is shown in Equation 14 below:

$$q_e = q_m * \exp(-K * \varepsilon^2) \quad \text{..... (14)}$$

Which can be linearized as:

$$Ln(q_e) = \ln(q_m) - K\,\varepsilon^2 \quad \text{..... (15)}$$

Where K is the Dubinin–Radushkevich isotherm constant. The value of ε can be determined from Equation 16 below (Dada et al., 2012):

$$\varepsilon = RT \ln(1+1/C_e) \quad \text{..... (16)}$$

To calculate the model coefficient (K) and the equilibrium uptake (q_m), lnq_e was plotted with e^2 (Equation 15) resulting in a slope (K) and the intercept ($\ln(q_m)$).

The results of Dubinin–Radushkevich isotherm model showed high fitting at pH 5 (R^2 = 0.94-0.95) and less fitting at a lower pH (R^2 = 0.77 -0.84). This result indicated that the adsorption process is homogenous, so the Dubinin–Radushkevich isotherm model provided poorer fitting compared to the Langmuir model, but was better than Freundlich model. The obtained q_m values are less than the experimental ones (C_o=160 ppm) with ratios of -18 %, - 22 %, -17 % at the temperatures of 25, 35, and 45 ºC, respectively (see Table 3).

Table 3. Calculated parameters of Dubinin–Radushkevich isotherm model at different temperatures and pH values

Temperature	pH= 3		pH =4		pH =5	
	R^2	q_m	R^2	q_m	R^2	q_m
25	0.80	6.83	0.77	10.48	0.94	17.67
35	0.88	8.76	0.79	12.34	0.95	19.02
45	0.84	10.41	0.78	17.76	0.95	19.70

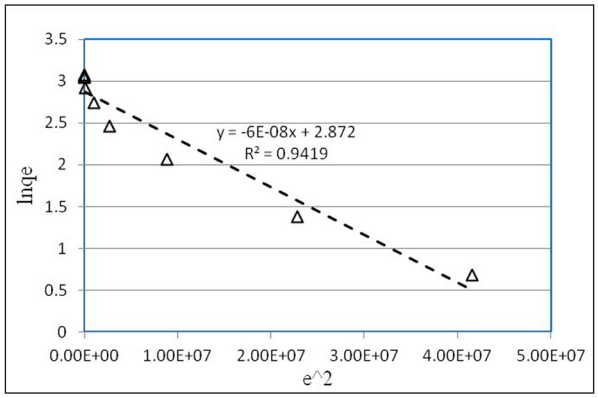

Figure 9. Validity of D-R model

3.8.4. Temkin Isotherm Model

This model takes in consideration the possible interaction between the geopolymer with chromium, where the heat of adsorption decreases linearly rather than logarithmically (Dada et al., 2012).

The linear form of Temkin isotherm model can be written as (Dada, 2012):

$$q_e = B\,lnA_T + B\,lnC_e \quad \text{..... (17)}$$

where B= RT/b_t, A_T is Temkin isotherm equilibrium binding constant (l/g); b_t: Temkin isotherm constant; B: Constant related to the heat of adsorption (J/mol);

The obtained data indicated a high correlation (>0.96) at all temperatures and pH values with better fitting at lower pH values (Table 4).

Table 4. Calculated parameters of Temkin isotherm model at different temperatures and pH values

Temperature	pH= 3			pH =4			pH =5		
	R^2	B	A_T	R^2	B	A_T	R^2	B	A_T
25	0.99	2.17	0.54	0.98	3.28	1.01	0.96	3.24	29.68
35	0.99	2.69	0.66	0.98	4.02	1.17	0.97	3.75	24.01
45	0.98	3.22	0.88	0.98	4.99	1.27	0.96	3.98	26.57

3.8.5. Calculation of Errors

The experimental q values were compared with the predicted model ones. MSE and χ^2 were calculated for each model as presented in table 5.

Based on the obtained results, the model's validity can be ranked according to MSE and χ^2 values as: Langmuir > Temkin > Frundilch > Dubinin–Radushkevich. It is worth mentioning that at pH=5, Dubinin–Radushkevich has better fitness than the Frundlich model.

Table 5. Calculated MSE and χ^2 for the isotherm models

	pH=3			pH=4			pH=5		
	R^2	MSE	χ^2	R^2	MSE	χ^2	R^2	MSE	χ^2
Langmuir	0.99	0.041	0.062	0.99	0.18	0.23	0.99	0.17	0.13
Frindluch	0.96	0.46	0.58	0.96	1.61	1.29	0.84	19.02	10.0
Dubinin–Radushkevich	0.8	1.97	3.02	0.77	7.65	7.30	0.94	6.61	3.94
Temkin	0.99	0.065	0.160	0.98	0.33	1.061	0.96	2.08	1.52

3.9. Kinetics of the Adsorption Process

The three time-dependent models mentioned above were used to determine the fitness of these models to the experimental data. The results suggest that the second order model provided the highest R^2 (0.97) against 0.44 and 0.62 for the first order and the intraparticle models, respectively (Figure 10). Although the 2nd order model has high fitness, it provided a lower estimate at a longer contact time; this could be attributed to the insignificant change in q_t after thirty minutes. contact time. Balan et al. (2009) indicated that the

adsorption of Cr^{+3} on the Sphagnum moss peat followed the pseudo-second order kinetic model, with R^2 >0.99, whereas, Meshram et al., (2012) found that the adsorption of Cr^{+3} by Amberlite IR 120 Resin has a good fitting ($R^2 \geq 0.97$) to the Lagergren first order model. Similar results were obtained by Al-Zboon et al. (2016); the second order obtained better fitness to the experimental data than the first order and intraparticle models.

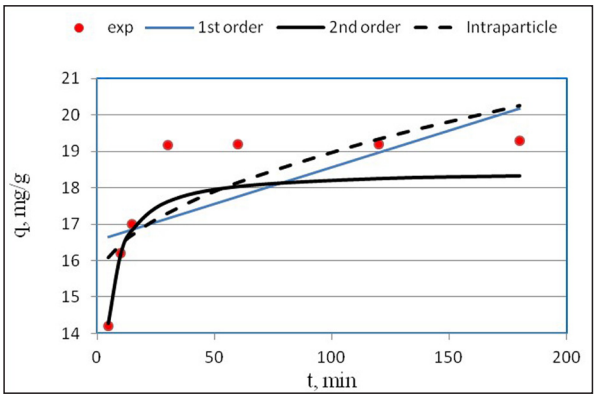

Figure 10. Validity of the kinetic models

3.10. Thermodynamic Study:

Table 6 shows that the distribution coefficient (K_d) values increased as pH and temperature increased. The higher value at higher temperatures and higher pH values indicate that a higher amount of metal is absorbed by the geopolymer (Al-Zboon et al., 2016).

The plot of $\ln K_d$ against 1/T yields a straight line with a slope of ΔH°, and an intersection of (ΔS^{o}). Gibbs free energy (ΔG^{o}) was determined by Equation 9 (see Table 6). The values of ΔH^{o} and ΔS^{o} ranged from 4.7 to 14.16 kJ/mol and 0.001 to 0.027 kJ/(mol.K) respectively. The positive sign of ΔH^{o} and ΔS^{o} and their decrease with the increase of pH buttress the favorability of the adsorption at higher pH. The positive value of ΔH^{o} suggests that ΔS^{o} of the system increases after the adsorption process.

The magnitude of ΔH^{o} provides an idea about the nature of adsorption, where the heat of physical adsorption ranges from 2.1–20.9 kJ/ mol, whereas, the heat of chemisorption generally ranges from 80 to 200 kJ/mol (Saha and Chowdhury, 2011). Therefore, it is concluded that the physio adsorption is the predominant process during Cr adsorption on geopolymer.

Table 6. Thermodynamic parameters calculated for Cr^{+3} adsorption on geopolymer

T, Kelvin	pH =3				pH=4				pH=5			
	R^2	ΔH^0	ΔS^0	ΔG^0	R^2	ΔH^0	ΔS^0	ΔG^0	R^2	ΔH^0	ΔS^0	ΔG^0
	-	kJ/ mol	kJ/ mol.K	kJ/ mol	-	kJ/ mol	kJ/ mol.K	kJ/ mol	-	kJ/ mol	kJ/ mol.K	kJ/ mol
298	0.98	14.16	0.027	6.01	0.98	8.58	0.012	5.73	0.97	4.70	0.001	5.46
308				5.02				4.90				4.78
318				4.40				4.39				4.38

The adsorption process has low affinity for the heterogeneous system as suggested by the low values of entropy (ΔS^{o}) (Al-Zboon et al., 2016). A positive value of ΔS^{o} mirrors the affinity of the adsorbent towards the adsorbate and increased randomness at the solid-solution interface with some structural changes in the adsorbate and the adsorbent (Saha and Chowdhury, 2011).

ΔG^{o} values decreased from 6.01 at T= 298 K, pH =3 to 4.38 at T = 318 K, pH=5 suggesting an endothermic process and more favorable at higher temperature (Saha and Chowdhury, 2011). The impact of pH on ΔG^{o} values decreased with the increase of temperature, where the difference becomes close to zero at temperature of 318 K indicating that temperature has a higher impact than pH (Figure 11).

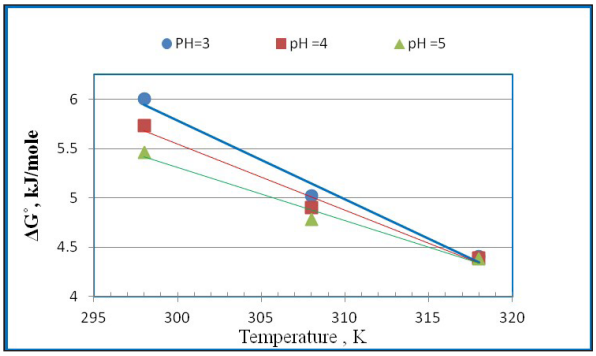

Figure 11. Relationship between temperature and ΔG^{o} values at different temperatures and different pH values

3.11. Activation Energy and Sticking Probability

The activation energy is the energy required for the ion to overcome or interact with the adsorbent surface (Saha and Chowdhury, 2011). The removal efficiency, the activation energy (E_a) and the sticking probability (S*) are indicators of the adsorption effectiveness where the direct relationship between them is shown in Equation 16 below (Ayawei et al., 2015):

$$\ln(1-\theta) = \ln S^* + E_a/RT \ldots \quad (18)$$

The plot of ln(1-θ) against 1/RT resulted in the slope of E_a, and intercept of S*. The positive value of E_a (28.54 kJ/mol at pH=5) suggesting that Cr adsorption by the geopolymer surface is a simple physical process, because the value of activation energy was in the range of 21 to 42 kJ/mol (Sismanoglu et al., 2004).

The calculated S* value was very low (<<<1) indicating a strong binding of the ions to the geopolymer surface (Saroj et al., 2013).

4. Conclusions

The current study focused on the adsorption of chromium (III) on volcanic tuff-based geopolymer from aqueous solutions. The impact of pH, contact time, dosage, and the adsorbent initial concentration on the performance of the adsorption process was investigated. An Isotherm study was conducted by applying four common models, while adsorption kinetic was investigated using three models. The results showed that the most applicable and feasible

conditions for the adsorption of Cr^{+3} on the synthesized geopolymer were: pH=5, contact time= thirty minutes. geopolymer dosage =0.25 g. Natural volcanic tuff-based geopolymer is capable of achieving a removal efficiency of 93.65 % with an uptake capacity of 19.3 mg Cr/g of geopolymer. The adsorption process followed the Langmuir isotherm model with less fitness to the Freundlich model. The second order kinetic model provided good fitness to the kinetic data. The thermodynamic study revealed that the adsorption process is endothermic and encouraged at a higher temperature. It is irreversible and physical with the ions being highly stuck to the geopolymer surface. The present study concludes that volcanic tuff-based geopolymer can be used as a low-cost adsorbent for the removal of metal ions from aqueous solutions.

References

Abdul Rahim, R.H., Rahmiati, T., Azizli, K.A., Man, Z., Nuruddin, M.F., Ismail, L. (2014). Comparison of Using NaOH and KOH Activated Fly Ash-Based Geopolymer on the Mechanical Properties. Materials Science Forum, 803: 179-184.

Al Bakri, A.M.M., Kamarudin, H., Bnhussain, M., Khairul, Nizar I., Rafiza, A.R., Zarina Y. (2012). The processing, characterization, and properties of fly ash based geopolymer concrete. Reviews on advanced materials science, 30(2012): 90-97.

Al Dwairi, R. (2017). Modeling of chromium (VI) adsorption from aqueous solutions using Jordanian Zeolitic Tuff. Water Sci Technol., 75(9-10): 2064-2071.

Al-Haj-Ali, A.M., and Marashdeh, L.M. (2014). Removal of Aqueous Chromium (III) Ions Using Jordanian Natural Zeolite Tuff in Batch and Fixed Bed Modes. Jordan Journal of Earth and Environmental Sciences, 6(2): 45- 51.

Al-Harahsheh, M.S., Al-Zboon, K., Al-Makhadmeh, L., Hararah, M., Mahasneh, M. (2015). Fly ash based geopolymer for heavy metal removal: A case study on copper removal. Journal of Environmental Chemical Engineering, 3(3): 1669–1677.

Al-Harahsheh, M.S., Shawabkeh, R., Batiha, M., Al-Harahsheh, A., Al-Zboon, K. (2014). Sulfur Dioxide Removal using Natural Zeolitic Tuff. Fuel Processing Technology, 126: 249–258.

Al-Tabbal, J., Al-Zboon, K., Al-Zouby, J., Al-Smadi, B., Ammary, B.Y. (2016). Effect of zeolux use on sage (salvia officinalis) plant irrigated by fresh and Ro reject waters. Global NEST Journal, 18(2): 416 - 425.

Álvarez-Ayuso, E., Querol, X., Plana, F., Alastuey, A., Moreno, N., Izquierdo, M., Font, O., Moreno, T., Diez, S., Vazquez, E., Barra, M. (2008). Environmental, physical and structural characterization of geopolymer matrixes synthesized from coal (co- combustion fly ashes. Journal of Hazardous Materials, 154(1–3), 175–183.

Al-Zboon, K., Al-Harahsheh, M., Falah, B.H. (2011). fly ash based geopolymer for Pb removal. Journal of Hazardous Materials, 188(1–3): 414–421.

Al-Zboon, K.K., Al-Smadi, B.M., Al-Khawaldah, S. (2016). Natural Volcanic Tuff-Based Geopolymer for Zn Removal: Adsorption Isotherm, Kinetic, and Thermodynamic Study. Water Air Soil Pollution, 227(7): 227-248.

Al-Zboon, K.K., and Al-Zou'by, J. (2016). Effect of volcanic tuff on the characteristics of cement mortar. European Journal of Environmental and Civil Engineering, 20(5): 520-531.

Al-Zou'by, J.Y., Al-Zboon, K., Al-Tabbal, J.A. (2013). Low-cost treatment of grey water and reuse for irrigation of home garden plants. Environmental Engineering and Management Journal, 16(2): 351-359.

Amenaghawon, N.A., Aisien, F.A., Agho, O.E. (2013). Application of Recycled Rubber from Scrap Tyres in the Adsorption of Toluene from Aqueous Solution. Journal of Applied Sciences and Environmental Management, 17(3): 411-417.

Anwar, J., Shafique, U., Salman, M., Waheed, uz Z., Anwar, S., Anzano, J.M. (2009). Removal of chromium (III) by using coal as adsorbent. Journal of Hazardous Materials, 171(1–3): 797–801.

Astutiningsih, S., and Liu, Y. (2005). Geopolymerization of Australian Slag with Effective Dissolution by the alkali, in Geopolymer: green chemistry and sustainable solution, Proceeding of Geopolymer Congress 2005, edited by Joseph Davidovits, Institute of Geopolymer, Paris, 69-73.

Ayawei, N., Inengite, A.K., Wankasi, D., Dikio, E.D. (2015). Synthesis and Sorption Studies of Lead (II) on Zn/Fe Layered Double Hydroxide. American Journal of Applied Chemistry, 3(3): 124-133.

Balan, C., Bilba, D., Macoveanu, M. (2009). Studies on chromium (III) removal from aqueous solutions by sorption on Sphagnum moss peat. Journal of the Serbian Chemical Society, 74 (8–9): 953–964.

Bansal, M., Singh, D., Garg, V.K., Rose, P. (2008). Mechanisms of Cr(vi) removal from synthetic wastewater by low cost adsorbents. Journal of Environmental Research and Development, 3(1): 228-243.

Bellú, S., García, S., González, J.C., Atria, A.M., Sala, L.F., Signorella, S. (2008). Removal of Chromium(VI) and Chromium(III) from Aqueous Solution by Grain–less Stalk of Corn. Separation Science and Technology, 43(11): 3200-3220 .

Chen, J., Wang, Y., Wang, H., Zhou, S., Wu, H., Lei, X. (2016). Detoxification/immobilization of hexavalent chromium using metakaolin-based geopolymer coupled with ferrous chloride. Journal of Environmental Chemical Engineering, 4(2): 2084–2089.

Chen, X. (2015). Modeling of Experimental Adsorption Isotherm Data. Information, 6: 14-22.

Cheng, T.W. (2003). Fire-Resistant Geopolymer Produced By Waste Serpentine Cutting, Proceedings of the 7th International Symposium on East Asian Resources Recycling Technology November 10-14, 2003, Tainan, 431-434.

Cheng, T.W., Lee, M.L., Ko, M.S., Ueng, T.H., Yang, S.F. (2012). The heavy metal adsorption characteristics on metakaolin-based geopolymer. Applied Clay Science, 56: 90-96.

Christiansen, M.U. (2013). An Investigation of Waste Glass-Based Geopolymers Supplemented with Alumina. Dissertation, Michigan Technological University.

Dada, A.O., Olalekan, A.P., Olatunya, A.M., Dada, O. (2012). Langmuir, Freundlich, Temkin and Dubinin–Radushkevich Isotherms Studies of Equilibrium Sorption of Zn Un to Phosphoric Acid Modified Rice Husk. IOSR Journal of Applied Chemistry, 3(1): 38-45.

Danielsson, L., and Söderberg, L. (2013). Removal of chromium in wastewater with natural clays in southern Malawi. Projektarbete 15hp, available at https://www.diva-portal.org/smash/get/diva2:619424/FULLTEXT01.pdf.

Dehghani, M.H., Sanaei, D., Ali, I., Bhatnagar, A. (2015). Removal of chromium(VI) from aqueous solution using treated waste newspaper as a low-cost adsorbent: Kinetic modeling and isotherm studies. Journal of Molecular Liquids, 215: 671–679.

Devi, R., and Kumar, H. (2015). Utilization of Waste Foundry Sand in Geopolymer Concrete. International Research Journal of Engineering and Technology, 2(2): 904-908.

Donat, R., Akdogan, A., Erdem, E., Cetisli, H. (2005). Thermodynamics of Pb2+ and Ni2+ adsorption onto natural bentonite from aqueous solutions. Journal of Colloid and

Interface Science, 286(1): 43–52.

El-Eswed, B., Alshaaer, M., Rushdi, I.Y., Hamadneh, I, Khalili, F. (2012). Adsorption of Cu(II), Ni(II), Zn(II), Cd(II) and Pb(II) onto Kaolin/Zeolite Based-Geopolymers. Advances in Materials Physics and Chemistry, 2 (4B): 119-125.

EPA, (2010). chromium-drinking-water, available at: https://www.epa.gov/dwstandardsregulations/chromium-drinking-water.

Foo, K.Y., and Hameed, B.H. (2010). Insights into the modeling of adsorption isotherm systems. Chemical Engineering Journal, 156(1): 2–10.

Ghazy S.E. , El-Asmy A.A., El-Nokrashy A.M. (2008). Separation of Chromium(III) and Chromium(VI) from Environmental Water Samples Using Eggshell Sorbent. Indian Journal of Science and Technology, 1(6): 1-7.

Ghazy, S.E. , El-Asmy, A.A. , El-Nokrashy, A.M. (2010). Removal of chromium(III) from water samples by a low-cost sorbent: application to a mixture of chromium(III) and chromium(VI)'. International Journal of Environmental Technology and Management. 12(2-4): 240-256.

Gupta S., and Babu B.V. (2008). Economic feasibility analysis of low cost adsorbents for the removal of Cr(VI) from waste water. Proceedings of International Convention on Water Resources Development and Management (ICWRDM), BITS Pilani, October 23-26.

Hamaideh, A., Al-Qarallah, B., Hamdi, R.M., Abu Mallouh, S.A., Al-Kafawein, J.K., Alshaaer, M. (2014). Synthesis of Geopolymers Using Local Resources for Construction and Water Purification. Journal of Water Resource and Protection, 6(5): 507-513.

Hanzlicek, T., Steinerova, M., Straka P. (2006). Radioactive Metal Isotopes Stabilized in a Geopolymer Matrix: Determination of a Leaching Extract by a Radiotracer Method. Journal of the American Ceramic Society, 89 (11), 3541–3543.

Hawley, E.L., Deeb, R.A., Kavanaugh, M.C., Jacobs, J.R.G. (2004). Treatment Technologies for Chromium (VI). In Chromium (VI) Handbook, Edited by Guertin, J., Jacobs, J. A., Avakian C. P., CRC Press, Boca Raton.

He, J., Jie, Y., Zhang, J., Yu, Y., Zhang, G. (2013). Synthesis and characterization of red mud and rice husk ash-based geopolymer composites. Cement and Concrete Composites, 37, 108–118.

Ibrahim, K.M. (2001). Evaluation of Jordanian faujasite tuff by comparison with other natural and synthetic zeolites. Environmental Geology, 40(4–5): 440–44.

Ibrahim, K.M., Khoury, H.N., Tuffaha, R. (2016). Mo and Ni Removal from Drinking Water Using Zeolitic Tuff from Jordan. Minerals, 6(116):6-13.

Jacobs, J., and Testa, S.M. (2004). Overview of Chromium (VI) in the Environment: Background and History. Chromium (VI) Handbook, available at: http://www.engr.uconn.edu/~baholmen/docs/ENVE290W/National%20Chromium%20Files%20From%20Luke/Cr(VI)%20Handbook/L1608_C01.pdf.

Janus, J.A., and Krajnc, E.I. (1990). Integrated criteria document chromium: effects. Appendix. Bilthoven, Netherlands. National Institute of Public Health and Environmental Protection, Springfield, VA : NTIS.

Kanwal, F., Imran, M., Mitu, L., Rashid, Z., Razzaq, H., Qurat-Ul-Ain. (2012). Removal of Chromium (III) Using Synthetic Polymers, Copolymers and their Sulfonated Derivatives as Adsorbents. E-Journal of Chemistry, 9(2): 621-630.

Khoury, H.N. (2014). Importance of Clay Minerals in Jordan Case Study: Volkonskoite as a Sink for Hazardous Elements of a High pH Plume. Jordan Journal of Earth and Environmental Sciences, 6(3): 1-9.

Krishna, D., and Sree, R.P. (2013). Removal of Chromium from Aqueous Solution by Custard Apple (Annona Squamosa) Peel Powder as Adsorbent. International Journal of Applied Science and Engineering, 11(2): 171-194.

Lancellotti, I., Kamseu, E., Barbieri, L., Corradi, A., Leonelli, C. (2011). Municipal solid waste incinerator fly ash to obtain geopolymers. Second International Volarization Symposium, 18-20 April 2011, Leuven Belgium.

Li, L., Wang, S., Zhu, Z. (2006). Geopolymeric adsorbents from fly ash for dye removal from aqueous solution. Journal of Colloid and Interface Science, 300(1): 52–59.

López, F.J., Sugita, S., Tagaya, M., Kobayashi, T. (2014). Metakaolin-Based Geopolymers for Targeted Adsorbents to Heavy Metal Ion Separation. Journal of Materials Science and Chemical Engineering, 02(07):16-27.

Luukkonen, T., Sarkkinen, M., Kemppainen, K., Rämö, J., Lassi, U. (2016). Metakaolin geopolymer characterization and application for ammonium removal from model solutions and landfill leachate. Applied Clay Science, 119(2): 266–276.

Meroufel, B., Benali, O., Benyahia, M., Zenasni, M.A., Merlin, A., George, B. (2013). Removal of Zn (II) from Aqueous Solution onto Kaolin by Batch Design. Journal of Water Resource and Protection, 5: 669-680.

Meshram, P., Sahu, S.K., Pandey, B.D., Kumar, V., Mankhand, T.R. (2012). Removal of Chromium(III) from the Waste Solution of an Indian Tannery by Amberlite IR 120 Resin. International Journal of Nonferrous Metallurgy, 1(3): 32-41.

Misra, A., Gupta, R., Gupta, R.C. (2003). Utilization of marble slurry in construction materials, Workshop on Gainful Utilization of Marble Slurry and Other Stone Waste. in: Indian School of Mines, available from: http://www.cdosindia.com.

Mohan, D., Singh, K.P., Singh, V.K. (2006). Trivalent chromium removal from wastewater using low cost activated carbon derived from agricultural waste material and activated carbon fabric cloth. Journal of Hazardous Materials, 135(1-3): 280–295.

Mužek, M.N., Svilović, S., Ugrina, M., Zelić, J. (2016). Removal of copper and cobalt ions by fly ash-based geopolymer from solutions-equilibrium study. Desalination and Water Treatment, 57(23): 10689-10699.

Nikagolla, C., Chandrajith, R., Weerasooriya, R., Dissanayake, C.B. (2013). Adsorption kinetics of chromium(III) removal from aqueous solutions using natural red earth. Environmental Earth Sciences, 68(3): 641–645.

Odeh, L., Odeh, I., Khamis, M., Khatib, M., Qurie, M., Shakhsher, Z., Qutob, M. (2015). Hexavalent Chromium Removal and Reduction to Cr (III) by Polystyrene Tris(2-aminoethyl)amine. American Journal of Analytical Chemistry, 6(1): 26-37.

Onutai, S., Jiemsirilers, S., Thavorniti, P., Kobayashi, T. (2015). Aluminum hydroxide waste based geopolymer composed of fly ash for sustainable cement materials. Construction and Building Materials, 101(1): 298–308.

Ouadjenia-Marouf, F., Marouf, R., Schott, J., Yahiaoui, A. (2013). Removal of Cu(II), Cd(II) and Cr(III) ions from aqueous solution by dam silt. Arabian Journal of Chemistry, 6(4): 401–406.

Pansini, M., Colella, C., De Gennaro, M. (1991). Chromium removal from water by ion exchange using zeolite. Desalination, 83(1–3): 145-157.

Rane, N.M., Sapkal, R.S., Sapkal, V.S., Patil, M.B., Shewale, S.P. (2008). Use of naturally available low cost adsorbents for removal of Cr (VI) from waste water. International Journal of Chemical Sciences and Applications, 1(2): 65-69.

Rangan, B.V. (2008). Low-Calcium Fly Ash-Based Geopolymer Concrete. Chapter 26, Concrete Construction Engineering

Handbook, Second Edition, Editor-in-Chief: E.G. Nawy, CRC Press, New York, 2008, pp. 26.1-26.20.

Saha, P., and Chowdhury, Sh. (2011). Insight Into Adsorption Thermodynamics. Book: Thermodynamics, Edited by Mizutani T., INTECH, available at: http://cdn.intechweb.org/pdfs/13254.pdf.

Sampranpiboon, P., Charnkeitkong, P., Feng, X. (2014). Equilibrium Isotherm Models for Adsorption of Zinc (II) ion from Aqueous Solution on Pulp Waste. Wseas Transactions on Environment and Development, 10: 35-47.

Sismanoglu, T., Ercag, A., Pura, S., Ercag, E. (2004). Kinetics and isotherms of dazomet adsorption on natural adsorbents. Journal of Brazilian Chemical Society, 15(15): 669-675.

Sqoor, S., Sarireh, M., Alahmer, A., Tarawneh, W. (2015). Feasibility of using volcanic tuff stone in ground heat exchange for cooling and heating Systems in buildings. International Journal of Thermal & Environmental Engineering, 9(1): 33-39.

Tangjuank, S., Insuk, N., Udeye, V., Tontrakoon, J. (2009). Chromium (III) sorption from aqueous solutions using activated carbon prepared from cashew nut shells. International Journal of Physical Sciences, 4(8): 412-417.

Tofan, L., Paduraru, C., Teodosiu, C., Toma, O. (2015). Fixed Bed Column Study on the Removal of Chromium (Iii) Ions from Aqueous Solutions by Using Hemp Fibers with Improved Sorption Performance. Cellulose Chemical. Technology, 49(2): 219-229.

WHO (2003). Chromium in Drinking-water, available at: https://www.who.int/water_sanitation_health/dwq/chemicals/chromium.pdf.

Yousef, N.S., Hazzaa, R., Farouq, R. (2015). Adsorptive Removal of Chromium (III) from Aqueous Solution Using Cation-Exchange Resin: Development of an Empirical Model. International Proceedings of Chemical, Biological and Environmental Engineering, 88(5): 21-28.